Proposed structure of putative glucose channel in GLUT1 facilitative glucose transporter

ARTICLE *in* BIOPHYSICAL JOURNAL · FEBRUARY 1996

Impact Factor: 3.97 · DOI: 10.1016/S0006-3495(96)79560-7 · Source: PubMed

Proposed Structure of Putative Glucose Channel in GLUT1 Facilitative Glucose Transporter

Hong Zeng, R. Parthasarathy,* Amrit L. Rampal, and Chan Y. Jung
Department of Biophysical Sciences, State University of New York at Buffalo, Biophysics Laboratory, Veterans Administration Medical Center, Buffalo, New York 14215; and *Biophysics Department, Roswell Park Cancer Institute, Buffalo, New York 14263 USA

ABSTRACT A family of structurally related intrinsic membrane proteins (facilitative glucose transporters) catalyzes the movement of glucose across the plasma membrane of animal cells. Evidence indicates that these proteins show a common structural motif where approximately 50% of the mass is embedded in lipid bilayer (transmembrane domain) in 12 α-helices (transmembrane helices; TMHs) and accommodates a water-filled channel for substrate passage (glucose channel) whose tertiary structure is currently unknown. Using recent advances in protein structure prediction algorithms we proposed here two three-dimensional structural models for the transmembrane glucose channel of GLUT1 glucose transporter. Our models emphasize the physical dimension and water accessibility of the channel, loop lengths between TMHs, the macrodipole orientation in four-helix bundle motif, and helix packing energy. Our models predict that five TMHs, either TMHs 3, 4, 7, 8, 11 (Model 1) or TMHs 2, 5, 11, 8, 7 (Model 2), line the channel, and the remaining TMHs surround these channel-lining TMHs. We discuss how our models are compatible with the experimental data obtained with this protein, and how they can be used in designing new biochemical and molecular biological experiments in elucidation of the structural basis of this important protein function.

INTRODUCTION

Glucose uptake by mammalian cells is a highly regulated process where selected monosaccharides are rapidly transported across the otherwise practically impermeable membrane diffusion barrier (Jung, 1975). Recent advances in gene cloning technology have revealed a family of structurally related, intrinsic membrane proteins (facilitative glucose transporters) that catalyze this process (Carruthers, 1990; Baldwin, 1993; Bell et al., 1993; Mueckler, 1994). Six functional isoforms (GLUT1, 2, 3, 4, 5, and 7) are now identified in this family, which is distinct in tissue distribution and in response to hormonal and metabolic regulations (Bell et al., 1990; Baldwin, 1993). Of these, GLUT1, abundant in human erythrocytes and transformed cell lines, is the only isoform currently available as a pure and functional protein (Kasahara and Hinkle, 1977; Baldwin et al., 1980). This isoform has been studied extensively for both transport mechanism and protein characterization.

Amino acid sequence data (Bell et al., 1990; Mueckler, 1994) indicate that the members of this protein family contain amino acids ranging in number from 492 to 528. The members show about 40% sequence homology, yet are essentially superimposible in a hydropathy plot. A hydrophobic moment analysis of the GLUT1 sequence (Mueckler et al., 1985) has predicted that this protein contains a large transmembrane domain of 12 α-helices long enough (19–21 residues) and hydrophobic enough to span the membrane lipid bilayer (transmembrane α-helices or TMHs, numbered 1 through 12, counting from the amino terminal end). Also, some TMHs, typically 2, 3, 4, 5, 7, 8, and 11, are amphipathic, each containing more than four polar amino acid residues (Fig. 1). This general transmembrane topology of GLUT1 has been validated experimentally (Cairns et al., 1987; Hresko et al., 1994).

Circular dichroism spectral data of purified GLUT1 (Chin et al., 1987) revealed that this protein contains 82% α-helix, 10% β-turns, and 8% random coil with no detectable β-sheet. The high α-helical content in this protein was also confirmed in IR studies (Alvarez et al., 1987), strongly suggesting that the transmembrane domain is largely, if not entirely, α-helical. Linear dichroism and Fourier transform infrared spectral measurements on oriented film of GLUT1 in vesicles indicate that all TMHs are nearly perpendicular to the plane of the membrane lipid bilayer (Chin et al., 1986).

The loops separating each TMH are hydrophilic. Tryptic digestion studies (Cairns et al., 1987) indicate that the long, 65-amino-acid residue loop connecting TMHs 6 and 7 (the central loop) is cytoplasmic. Similarly, both the N- and C-terminal segments of 12- and 42-amino-acid residues, respectively, are also cytoplasmic. However, the glycosylated loop of 35 residues separating TMHs 1 and 2 is exoplasmic. Other loops are short, ranging from 7 to 14 residues. The loop sizes and the ends of helices, however, are not determined with any certainty.

The transmembrane domain is highly conserved among different isoforms and most likely accommodates a water-filled glucose channel that is common to all of the isoforms. Hydrogen-tritium and hydrogen-deuterium exchange data obtained from purified GLUT1 (Jung et al., 1986) and GLUT1-catalyzed water transport (Fischbarg et al., 1990) are indeed consistent with the presence of an aqueous chan-

Received for publication 5 May 1995 and in final form 21 September 1995.
Address reprint requests to Dr. Chan Y. Jung, the Biophysics Laboratory, Veterans Administration Medical Center, Buffalo, NY 14215. Tel.: 716-862-3309; Fax: 716-862-3419; E-mail: camcjung@ubvms.buffalo.cc.edu.

0006-3495/96/01/14/08 $2.00

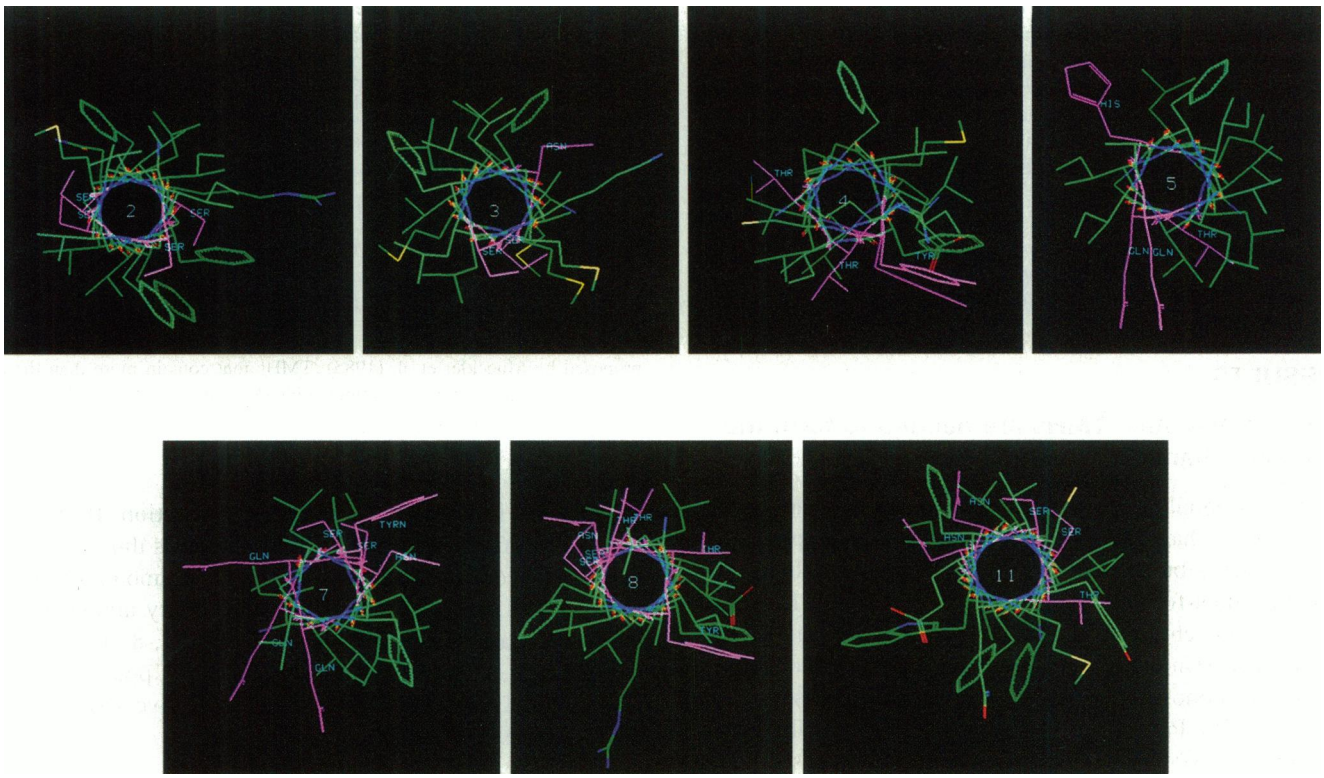

FIGURE 1 Helical wheel plots of the amphipathic TMHs 2, 3, 4, 5, 7, 8, 11. Polar residues are shown in purple, carbons in green, hydrogens in white, nitrogens in blue, oxygens in red.

nel in this protein. The nonmembrane domain, on the other hand, shows a significant isoform-specific amino acid sequence and may play an important role in the tissue-specific regulation of glucose transporter function.

The tertiary structure of the transmembrane domain involved in the translocation of glucose and other selected substrates has yet to be elucidated. Because of the technical difficulty of growing high-quality membrane protein crystals, direct x-ray structural determination of GLUT1 does not seem feasible immediately, and conventional biochemical or molecular biological dissection is the only practical approach to this problem. In the present study, we generate low-resolution structural models of the transmembrane domain of GLUT1 to assist this approach. Such computer model building has been successful in predicting low-resolution structures of the proteins, particularly those that are all α-helical (Cohen et al., 1979). We propose here two models for GLUT1 transmembrane domain glucose channel structure. Our models will be useful in designing biochemical and molecular biological experiments to understand the structural basis of GLUT1 and other facilitative glucose transporter function.

MATERIALS AND METHODS

We applied a heuristic approach to fit the following structural highlights known for GLUT1 protein: 1) The monomer is functional (Baldwin et al., 1981; Burant and Bell, 1992). 2) The transmembrane domain is made of 12 α-helices (TMHs), some of which are amphipathic, containing four or more polar residues (Fig. 1). 3) Five TMHs line a water-filled glucose channel. 4) The short loops, made of 7–14 hydrophilic residues, limit the relative position of connecting TMHs, whereas the long cytoplasmic loop between TMH 6 and 7 and the exoplasmic loop between TMH 1 and 2 do not. 5) Both the N- and the C-terminal are cytoplasmic. 6) All TMHs are oriented nearly normal to the bilayer.

The method consists of six major steps: (i) create the geometry for the TMHs 1–12 as α-helices, (ii) examine the lengths of the loops connecting the helices to decide their relative dispositions, (iii) assemble and arrange the helices as a four-helix bundle with their helix axes nearly parallel, (iv) decide on the relative orientation of the helices as parallel or antiparallel by considering macrodipole interactions, (v) create an aqueous glucose channel using five amphipathic TMHs, and finally (vi) select and refine several possible structures.

The amino acid sequences for 12 TMHs used here are those predicted by Mueckler et al. (1985): TMH1 (Met13-Ile33), TMH2 (Leu67-Val87), TMH3 (Met96-Gly116), TMH4 (Phe127-Val147), TMH5 (Leu156-Leu176), TMH6 (Trp186-Phe206), TMH7 (Ile272-Tyr292), TMH8 (Val307-Val327), TMH9 (Leu338-Leu358), TMH10 (Ile369-Phe389), TMH11 (Ala402-Phe422), TMH12 (Gly430-Phe450). Each helix was generated as a classical α-helix using the molecular mechanics package of Insight II V2.30 with Biopolymer Module (Biosym Technologies, San Diego, CA). The torsional angles were adjusted to the desired backbone and side-chain conformations (Vega et al., 1992; Lupas et al., 1994). Energy minimization, using Discover V3.1 (Biosym Technologies), was carried out for each helix after connecting each loop between helices by tethering the helices. This resulted in optimized packing within the local minima associated with the starting conformation. The minimization procedure typically consisted of two steps. First, structures were subjected to 100 steps of Steepest descents algorithm (Fletcher, 1980) to eliminate the worst steric conflicts. Subsequently, minimization using the Conjugate Gradient or Newton-Raphson algorithm (Fletcher, 1980) with no Morse

and no Crose was carried out until the norm of the gradient was less than 10^{-10}. The conjugate gradient method gave lower energy values for every one of the helices. TMHs 2 and 8 had lower energy, and TMHs 11 and 12 had relatively higher energy. The helical parameters were not constrained, and the helices were allowed to change from the starting values. In most cases, the helices remained intact, although a few residues exhibited some distortions from the ideal helical geometry.

Molecular dynamics trajectory calculations (Verlet, 1967; Discover V3.1, Biosym Technologies) were carried out after filling the channel with water molecules at constant pressure under conditions identical with those described for minimization. Simulations were run with an integration step of 1 fs at a temperature of 310 K for 10 ps of real time.

RESULTS

Five amphipathic TMHs are needed to form the glucose channel

It was essential to determine how many helices are needed to form the channel for glucose passage. For the passage of small ions, a bundle of four α-helices seems to be a plausible channel-forming element (Montal, 1990), whereas for the nicotinic cholinergic receptor, an array of five helices is implicated (Unwin, 1993). Facilitated glucose transporters transport monosaccharide but cannot transport disaccharide (Jung, 1975). Preliminary model building (B. H. Jhun et al., unpublished observations) and dimensional analysis of substrate and nonsubstrate sugars (Table 1) suggested that the channel formed by five helices in contact with one another will give a channel large enough for a hexose to pass through but not for a disaccharide. Four helices were unable to form a channel large enough for glucose passage, whereas six helices gave a channel large enough to fit a disaccharide. However, another arrangement of six helices could give a channel fit to monosaccharide only. As a first approximation, we chose to use five helices in this study.

Evidence indicates that the glucose channel is accessible to solvent water (Jung et al., 1986). It is well known that for water-soluble proteins a significant portion (47% in average) of their solvent-accessible surface represents polar residues (Miller et al., 1987). Furthermore, ample evidence indicates that hydrogen bonding between glucose and channel residues is essential for this protein function (Barnett et al., 1973; Jung, 1975; Carruthers, 1990). It is thus expected that the glucose channel contains a certain amount of polar residues and includes hydroxyls and primary amides (glutamine and asparagine). TMHs 2, 3, 4, 5, 7, 8, and 11 are amphipathic, each containing four or more polar residues (Fig. 1 and Table 2). The channel-forming five TMHs were among these TMHs.

TABLE 1 Dimensional analysis of GLUT1 substrates and permeability characteristics

Species	Physical dimensions (A)			Permeability‡
	Height*	Width*	Depth*	
D-Glucose	5.3	8.3	9.8	Permeable
D-Galactose	6.3	7.8	9.3	Permeable
D-Mannose	5.9	8.0	8.9	Permeable
Maltose	6.8	10.8	14.1	Impermeable
Cellobiose	6.8	10.9	16.4	Impermeable
Lactose	6.0	11.1	14.1	Impermeable
Sucrose	7.5	10.9	12.8	Impermeable
Gentiobiose	8.8	9.6	15.6	Impermeable
Trehalose	9.4	10.6	14.1	Impermeable
Melibiose	7.2	10.2	13.6	Impermeable

*Unpublished data by Jhun et al.
‡Data from Jung (1975).

TABLE 2 The amphipathic TMHs and distribution of hydrophilic residues that may line the putative glucose channel of GLUT1

TMH	Polar residues	Models
2	Ser68, **Ser73, Ser80,** Ser82	2
3	Asn100, **Ser106, Ser113,** Lys114	1
4	**Tyr132, Thr136,** Thr137, **Tyr143**	1
5	**Thr158,** His160, **Gln161, Gln172**	2
7	Gln279, **Ser281,** Gln282, Gln283, **Ser285, Asn288, Tyr292**	1 & 2
8	Tyr308, **Thr310, Ser313, Asn317,** Thr318, **Thr321, Ser324**	1 & 2
11	Ser410, **Asn411,** Thr413, **Ser414, Asn415**	1 & 2

Data are from the amino acid sequence and transmembrane topology proposed by Mueckler et al. (1985). TMHs that contain more than three polar residues are considered amphipathic. Residues exposed to the channel are shown in bold letters.

Relative disposition of the TMHs

The next problem was to find the relative dispositions of the helices. Because all TMHs are thought to be nearly perpendicular to the membrane surface (Chin et al., 1987), they must be positioned such that their helix axes vectors are either parallel or antiparallel. Some of these arrangements could be ruled out based on the lengths of the loops connecting the adjacent helices. The predicted lengths of the loops in GLUT1 (Mueckler et al., 1985) are, respectively, 33, 8, 10, 8, 9, 65, 14, 10, 10, 12, and 7 residues connecting successive helices starting from TMH 1 through TMH 12, although the actual loop sizes may vary by one or two amino acids either way. Short loops will exercise some stereochemical restrictions (Cohen et al., 1979); very long loops, on the other hand, may have structural significance. Furthermore, parallel helix vector orientation demands a long loop, which has to go across the membrane, whereas a short loop would suffice for antiparallel orientation.

Loop sizes connecting helices in protein structures

To solve the problem of whether the loop size between these helices in GLUT1 are long enough to form the antiparallel helix-helix interactions, we carried out a study of globular proteins of known structure that contain an antiparallel arrangement of helices. We studied the distribution of loops actually found in established protein structures listed in the Brookhaven Protein Data Bank. We eliminated structures that belong to the same family of proteins. Helices less than 14 residues in length were not considered. In the remaining

90 structures examined, we further limited the antiparallel helix-helix interaction angles to 180° ± 25°. We found that a loop size of four is the most frequent (Fig. 2 *A*). This would indicate that the nine short loop sizes in the GLUT1 structure correspond to antiparallel helical orientations and would not allow parallel orientation. However, the long central loop of 65 residues can readily accommodate the parallel orientation of TMH6 and TMH7 if required. It may be relevant to note in this regard that TMHs 1 through 6 and TMHs 7 through 12 may result from gene duplication and represent two separate domains in three-dimensional structure.

The interhelical distance for antiparallel helices

Using the Brookhaven Protein Data Bank for the globular proteins of known structure that contain an antiparallel arrangement of helices, we measured the distance between the centers of adjacent helices. The results (Fig. 2 *B*) strongly indicate that adjacent helices are in van der Waals contact. We modeled with several different initial distances between two adjacent helices, and selected the one with the lowest helical backing energy. These gave mean distances between the centers of adjacent helices of 11.1 Å (Model 1) and 11.5 Å (Model 2).

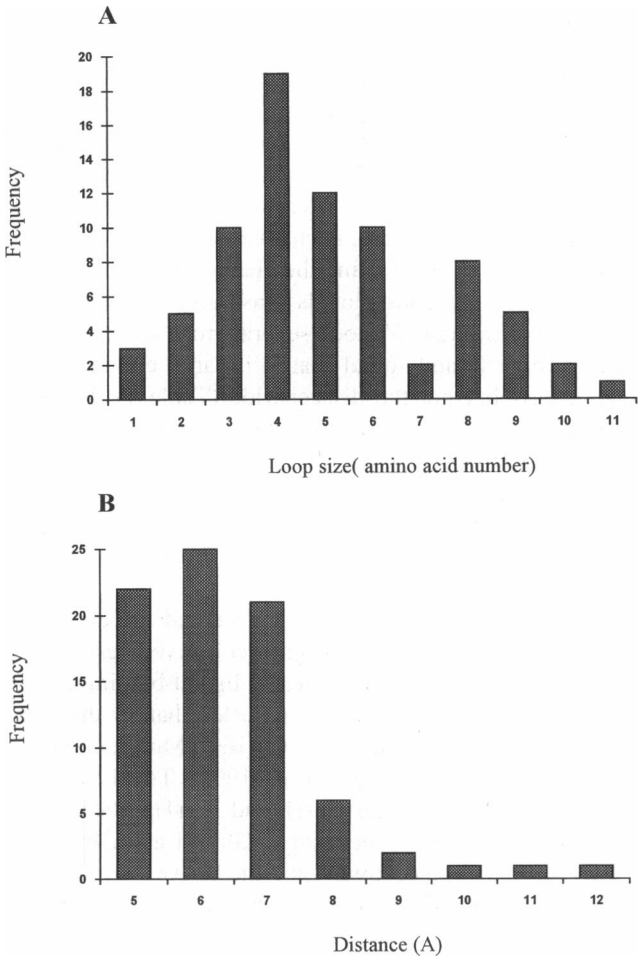

FIGURE 2 Interhelical loop sizes and interherical distances in the globlar proteins. (*A*) Number of occurrences (*y* axis) of loops versus the number of amino acid residues (*x* axis) in loops that connect two antiparallel helices (see Materials and Methods for details). (*B*) Number of occurrences (*y* axis) of a given interhelical distance measured center to center of adjacent helices (*x* axis) connected by the loops. The data were generated from the Brookhaven Protein Data Bank using INSIGHT II.

Effects of a macrodipole on relative helix orientations

The effects of a macrodipole due to a helix on a variety of biochemical phenomena (Wada, 1976; Hol, 1985) have been discussed, including the stability of four-helix bundles (Sheridan et al., 1982; Presnell and Cohen, 1989). In arranging the relative positions of TMHs, we noted an additional (although relatively small, amounting to 0.6 kcal/mol/pair) electrostatic stabilization provided by macrodipoles in antiparallel orientations of four-helix bundles (Robinson and Silgar, 1993).

Assembly of helices into four-helix bundles

After these background constraints were considered, we found that only two distinct TMH assemblies are possible (Fig. 3). In one (Model 1) TMHs 3, 4, 7, 8, and 11 were arranged to form the channel. In another (Model 2) TMHs 2, 5, 11, 8, and 7 were used to form such a channel. Each of these helices could be turned about its own helical axis arbitrarily to produce enough polar residues (ranging from 30% to 80%) lining the channel. TMHs were then placed in such a way as to form three four-helix bundles. In these bundles, the helices are all nearly parallel; this square type of arrangement of helices occurs frequently in proteins (Harris et al., 1994). In Model 1 (Fig. 3 *a*) TMHs 1, 2, 3, and 12 formed one four-helix bundle; other two bundles are TMHs 4, 5, 6, 7 and TMHs 8, 9, 10, 11. These four-helix bundles are brought together to form an aqueous channel for glucose passage. As we go from the amino to the carboxyl end, TMH 1 points up (exoplasmic direction), TMH 2 points down (cytoplasmic direction), and so on until TMH 12, which points to the cytoplasm; they alternate pointing up and down. As a result, the four-helix bundles have adjacent helices antiparallel, resulting in favorable helix macrodipole interactions in each bundle. However, when the bundles are brought together, there is one unfavorable interaction, namely between TMHs 3 and 11. In Model 2 (Fig. 3 *b*), where TMHs 2, 5, 11, 8, and 7 were used to form the channel, the three four-helix bundles are TMHs 2, 3, 4, and 5 forming one bundle; TMHs 5, 6, 12, and 11 forming the second bundle; and TMHs 11, 10, 9, and 8 forming the third bundle. The bundle formation is very different in the two models. In Model 1 (Fig. 3 *a*), adjacent TMHs in sequence form the bundles. In Model 2 (Fig. 3 *b*), TMHs far apart in sequence come together to form bundles, and TMHs 5 And 11 play a double role, occurring twice in bundle

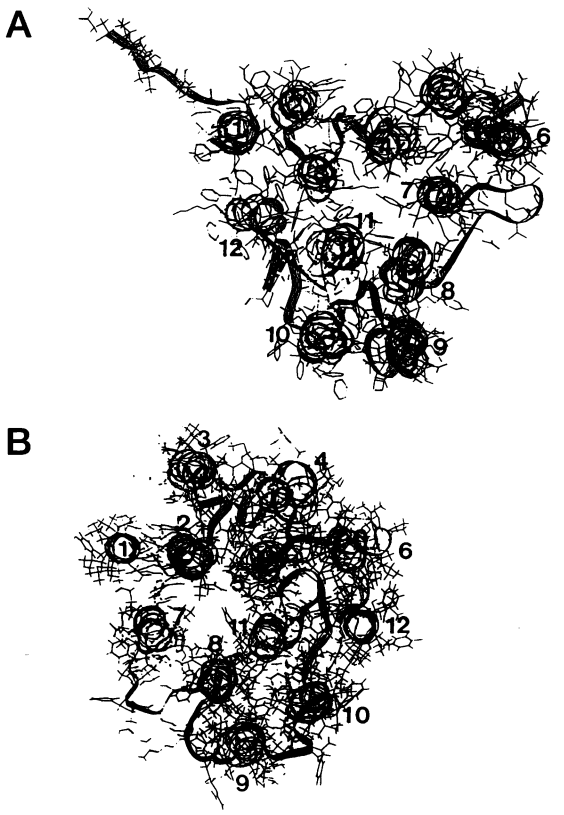

FIGURE 3 Arrangement of TMHs in the transmembrane domain and glucose channel after energy minimization. Exoplasmic view for Model 1 (*a*) and Model 2 (*b*). Individual TMHs are identified by 1 through 12 counting from the amino terminus.

formation. In this model, furthermore, the long central loop between TMHs 6 and 7 is used as an important structural feature; it places TMH 7 far from TMH 6 and near TMH 2 and 1. This model gives rise to a bilobular symmetry in three dimensions, as reflected in the hydropathy profile. The TMH orientations alternate in their macrodipole orientation: 1 up, 2 down, and so on up to 12 down. As before, all of the odd ones point outside, and the even ones point inside. As for the first model, the four-helix bundles have adjacent helices pointing antiparallel, resulting in favorable helix macrodipole interactions in each bundle. However, when the bundles are brought together, there is, as in Model 1, one unfavorable interaction between TMH helices 5 and 11.

Refinement of models

The two models discussed above were considered worthy of further refinement. Energy minimization was performed after interhelical loop connection, except that the conformation of the two long loops (between TMHs 1 and 2, and between TMHs 6 and 7) was not considered. Energy minimization and molecular dynamic (Biosym 1993) simulations were carried out after filling the channel with water molecules and setting the temperature at 310 K; other parameters were set as default. Dynamics and possible fine structural modulation involving the oligomeric assembly of GLUT1 (Carruthers, 1990; Herbert and Carruthers, 1992) were not considered in these models.

DISCUSSION

The two models proposed here for the tertiary structure of GLUT1 transmembrane domain (Fig. 3, *a* and *b*, for Models 1 and 2, respectively) have many redeeming features and fit many biophysical and biochemical observations made with this protein. Model 2 may have an edge, as it incorporates a possible structural significance of the long loop between TMHs 6 and 7 and has a bilobular symmetry. The models describe only the relative disposition of the transmembrane helices. Our models indicate that the molecule is fairly compact. All of the transmembrane helices are nearly normal to the membrane and are parallel. The loops serve the purpose mainly of limiting the distance at which the connecting helices can be kept apart.

In both of our models, the channel is reasonably (40%-60%) hydrophilic (Table 2), consistent with the suggested presence of an aqueous channel within the protein (Jung et al., 1986; Alvarez et al., 1987; Fischbarg et al., 1990). The channel in both models contains several amino acid residues capable of hydrogen-bond formation with glucose (Table 2). In either models, the N-terminal half provides two TMHs directly participating in channel formation. The more polar TMHs 7, 8, and 11 line the channel in both models.

The channel in both models was large enough to let glucose pass through. We took several cross sections of the channel (Fig. 4) and found that it is large enough to let glucose pass but not the disaccharide (Table 1). We also examined a computer-drawn longitudinal cut of the channel (Fig. 5) and found no major obstruction for the glucose molecule for the entire length of the channel. In the dynamic state of the protein, however, channels can become bigger or smaller momentarily, and we did not focus on this aspect of the problem.

More recently, investigators have studied the effects of site-directed mutagenesis of highly conserved residues of GLUT1 on its transport and external ligand-binding activities. The results of these studies revealed that, of the more than 12 residues studied, four, Gln161 (Mueckler et al., 1994), Gln282 (Hashiramoto et al., 1992), Trp412 (Garcia et al., 1992; Katagiri et al, 1991), and Asn415 (Ishihara et al., 1991), were found to be critical. Gln161 and Gln282 lie in TMHs 5 and 7, respectively, and the last two are in TMH 11. All of these TMHs form the channel in our Model 2, although TMH 5 does not participate in channel formation in Model 1 (Fig. 3). Furthermore, Gln161, Gln282, and Asn415 line the channel in our models, whereas Trp412 may be critical for proper channel conformation because of its interaction with Asn411 (Table 2). The predictions for channel-lining residues, however, have no rigorous basis in our models at this stage. Possible involvement of three proline residues in TMH 10 in transport activity has been

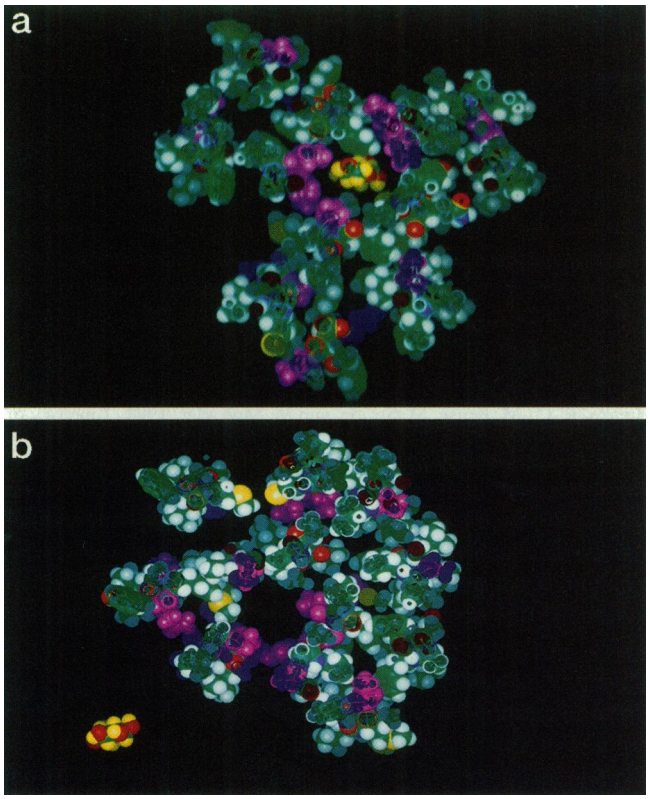

FIGURE 4 A cross section of the channel. Carbon is shown in green, hydrogen in white, nitrogen is in blue, oxygen in red, sulfur in yellow, and polar residues in purple. The D-glucose molecule is also included for comparison of its size to that of the channel. Hydrogens in the glucose molecule are shown in yellow rather than white. Membrane plane cross section of Model 1 (*a*) and Model 2 (*b*), at $z = 14$ (14 Å from exoplasmic surface into the channel), are shown.

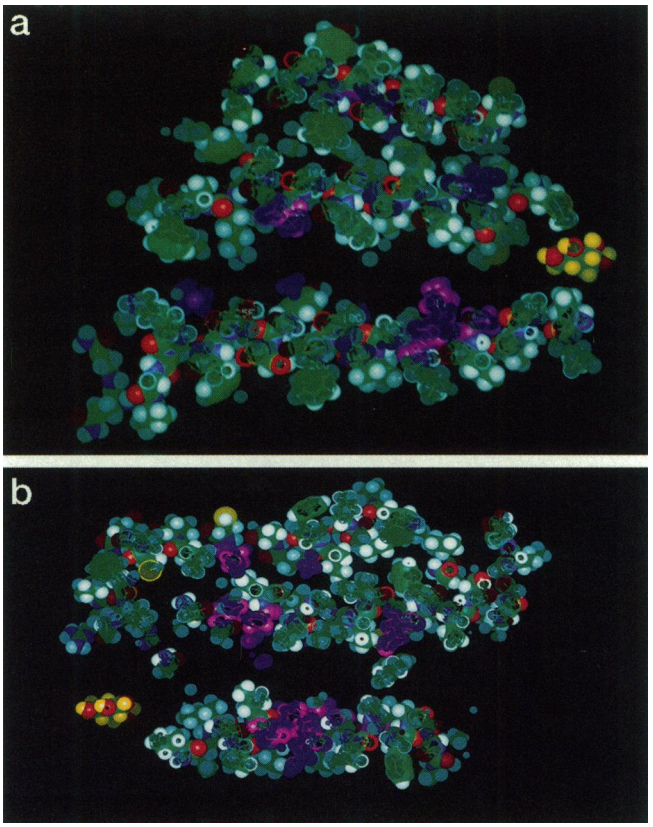

FIGURE 5 A longitudinal cross section of the channel. The same color codes are used here as in Figs. 1 and 4. The D-glucose molecule (*yellow*) is also included for comparison of its size to that of the channel. (*a*) Model 1: TMHs 1, 3, and 7 (*top to bottom*); exoplasmic (*right side*) and cytoplasmic (*left side, with glucose molecule*). (*b*) Model 2: TMHs 6, 5, and 7 (*top to bottom*) are shown with the exoplasmic end at right and the cytoplasmic end at left.

indicated (Tamori et al., 1994; Wellner et al., 1995), although its structural implication with regard to the glucose channel is less clear.

Our two models predict distinct interhelical positional relationships that can be tested experimentally. For example, using cysteine site-directed mutagenesis and pyrene labeling (Jung et al., 1993; see also Due et al., 1995), the proximity of TMH 6 to TMH 7 or TMH 12 can be determined. In Model 1, TMH 6 is next to TMH 7, whereas in Model 2, it is next to TMH 12 and not TMH 7. The two models also differ in channel-lining TMHs (TMHs 3 and 4 for Model 1, and TMHs 2 and 5 for Model 2) and predict distinct amino acid residues that are exposed to the channel (Table 2). Some of these residues may be essential for transport function through hydrogen bond formation with a substrate. It is interesting to see how mutation of each of these channel-lining residues affects transporter function.

Recently, several structural models have been proposed for GLUT1. Gould and Holman (1993) quote a hypothetical helix packing model for GLUT1, but its details were not given. Baldwin (1993) described two speculative helix packing schemes, one forming the channel between six helices (TMHs 1, 5, 6, 7, 11, and 12), and the other forming the channel between four helices (TMHs 7, 8, 10, and 11). These models, however, consider no physical dimension or chemical requirements of the channel for substrate passage. Very recently, Fischbarg et al. (1993) have proposed the possibility that glucose transporters may fold as β-barrels. However, this model totally ignores the extensive biochemical and molecular biological data that support the GLUT1 transmembrane topology consisting of 12 transmembrane segments (Baldwin, 1993; Hresko et al., 1994; Mueckler, 1994). Furthermore, the spectral data currently available (Chin et al., 1987; Alvarez et al., 1987) do not support the presence of β-sheets in quantity, which would be required for the barrel structure in this protein.

This work was supported in part by grant DK-13376 from the National Institutes of Health and by the Veterans Administration Medical Center, Buffalo, New York.

REFERENCES

Alvarez, J., D. C. Lee, S. A. Baldwin, and D. Chapman. 1987. Fourier transform infrared ectroscopic study of the structure and conformational

changes of the human erythrocyte glucose transporter. *J. Biol. Chem.* 262:3502–3509.

Baldwin, J. M., G. E. Linehard, and S. A. Baldwin. 1980. The monosaccharide transport system of the human erythrocyte. *Biochim. Biophys. Acta.* 599:699–714.

Baldwin, S. A. 1993. Mammalian passive glucose transporters: members of an ubiquitous family of active and passive transport proteins. *Biochim. Biophys. Acta.* 1154:17–49.

Baldwin, S. A., J. C. Gorga, and G. E. Lienhard 1981. The monosaccharide transporter of the human erythrocyte. Transport activity upon reconstitution. *J. Biol. Chem.* 256:3685–3689.

Barnett, J. E. G., G. D. Holman, and K. A. Munday. 1973. Structural requirements for binding to the sugar transport system of the human erythrocyte. *Biochem. J.* 131:211–221.

Bell, G. I., C. F. Burant, J. Takeda, and G. W. Gould. 1993. Structure and function of mammalian facilitative sugar transporters. *J. Biol. Chem.* 268:1961–1964.

Bell, G. I., T. Kayano, J. B. Buse, C. F. Burant, J. Takede, D. Lin, H. Fukumoto, and S. Seino. 1990. Molecular biology of mammalian glucose transporters. *Diabetes Care.* 13:198–208.

Burant, C. F., and G. I. Bell. 1992. Mammalian facilitative glucose transporters: evidence for similar substrate recognition sites in functionally monomeric proteins. *Biochemistry.* 31:10414–10420.

Cairns, M. T., J. Alvarez, M. Panico, A. F. Giggs, H. R. Morris, D. Chapman, and S. A. Baldwin. 1987. Investigation of the structure and function of the human erythrocyte glucose transporter by proteolytic digestion. *Biochim. Biophys. Acta.* 905:295–310.

Carruthers, A. 1990. Facilitated diffusion of glucose. *Physiol. Rev.* 70: 1135–1172.

Chakrabarti, P. 1994. An assessment of the effect of the helix dipole in protein structures. *Protein Eng.* 7:471–474.

Chin, J. J., E. K. Y. Jung, V. Chen, and C. Y. Jung. 1987. Structural basis of human erythrocyte glucose transporter function in proteoliposome vesicles: circular dichroism measurements. *Proc. Natl. Acad. Sci. USA.* 84:4113–4116.

Chin, J. J., E. K. Y. Jung, and C. Y. Jung. 1986. Structural basis of human erythrocyte glucose transporter function in reconstituted vesicles. *J. Biol. Chem.* 261:7101–7104

Cohen, F. E., T. J. Richmond, and F. M. Richards. 1979. Protein folding: evaluation of some simple rules for the assembly of helices into tertiary structures with myoglobin as an example. *J. Mol. Biol.* 132:275–288.

Cope, D. L., G. D. Holman, S. A. Baldwin, and A. J. Wolstenholme. 1994. Domain assembly of the GLUT1 glucose transporter. *Biochem. J.* 300: 291–294.

Due, A. D., J. A. Cook, S. J. Fletcher, Q. Z. Chao, A. C. Powers, and J. M. May. 1995. A systeineless GLUT1 glucose transporter has normal function when expressed in Xenopus oocytes. *Biochem. Biophys. Res. Commun.* 208:590–596.

Fasman, G. D., and W. A. Gilbert. 1990. The prediction of transmembrane protein sequences and their conformation: an evaluation. *Trends Biochem. Sci.* 15:89–92.

Fischbarg, J., M. Cheung, F. Czegledy, J. Li, P. Iserovich, K. Kuang, J. Hubbard, M. Garner, O. M. Rosen, D. W. Golde, and J. C. Vera. 1993. Evidence that facilitative glucose transporters may fold as beta-barrels. *Proc. Natl. Acad. Sci. USA.* 90:11658–11662.

Fischbarg, J., K. Y. Kuang, J. C. Vera, S. Arant, S. C. Silverstein, J. Loike, and O. M. Rosen. 1990. Glucose transporters serve as water channels. *Proc. Natl. Acad. Sci. USA.* 87:3244–3247.

Fletcher, R. 1980. Unconstrained optimization. *In* Practical Methods of Optimization, Vol. 1. Wiley and Sons, Chichester, England.

Fukumoto, H., S. Seino, H. Imura, Y. Seino. 1988. Characterization and expression of human HepG2/erythrocyte glucose-transporter gene. *Diabetes.* 37:657–661.

Garcia, J. C., M. Strube, K. Leingang, K. Keller, and M. Mueckler. 1992. Amino acid substitutions at tryptophan 388 and tryptophan 412 of the HepG2 (GLUT1) glucose transporter inhibits transport activity and targetting to the plasma membrane in Xenopus oocytes. *J. Biol. Chem.* 267:7770–7776.

Gould, G. W., and G. D. Holman. 1993. The glucose transporter family: structure, function and tissue-specific expression. *Biochem. J.* 295: 329–341.

Harris, N. L., S. R. Presnell, and F. E. Cohen. 1994. Four helix bundle diversity in globular proteins. *J. Mol. Biol.* 236:1356–1368.

Hashiramoto, M., T. Kadowaki, A. E. Clark, A. Muraoka, K. Mommura, H. Sakura, K. Tobe, Y. Akanuma, Y. Yazaki, G. D. Holman, and M. Kasuga. 1992. Site-directed mutagenesis of GLUT1 in Helix 7 residue 282 results in pertubation of exofacial ligand binding. *J. Biol. Chem.* 267:17502–17507.

Herbert, D. N., and A. Carruthers. 1992. Glucose transporter oligomeric structure determines transporter function. *J. Biol. Chem.* 267: 23829–23838.

Hol, W. G. J. 1985. The role of the alpha-helix dipole in protein function and structure. *Prog. Biophys. Mol. Biol.* 45:149–195.

Hresko, R. C., M. Kruse, M. Strube, and M. Mueckler. 1994. Topology of the Glut1 glucose transporter deduced from glycosylation scanning mutagenesis. *J. Biol. Chem.* 269:20482–20488.

Ishihara, H., T. Asano, H. Katagiri, J. L. Lin, K. Tsukuda, Y. Shibasaki, Y. Yazaki, and Y. Oka. 1991. The glucose transport activity of GLUT1 is markedly decreased by substitution of a single amino acid with a different charge at residue 415. *Biochem. Biophys. Res. Commun.* 176: 922–930.

Jung, C. Y. 1975. *In* The Red Blood Cells, Vol. 2. D. M. Surgenor, editor. Academic Press, New York. 705–711.

Jung, E. K. Y., J. J. Chin, and C. Y. Jung. 1986. Structural basis of human erythrocyte glucose transporter functions in reconstituted system. *J. Biol. Chem.* 261:9155–9160.

Jung, K., H. Jung, J. Wu, G. G. Prive, and H. R. Kaback 1993. Use of site-derected fluorescence labeling to study proximity relationships in the lactose permease of *E. coli. Biochemistry.* 23:12273–12278.

Kasahara, M., and P. C. Hinkle. 1977. Reconstitution and purification of the D-glucose transporter from human erythrocytes. *J. Biol. Chem.* 252:7384–7390.

Katagiri, H., T. Asano, Y. Shibasaki, J. L. Lin, K. Tsukuda, H. Ishihara, Y. Akanuma, F. Takaku, and Y. Oka. 1991. Substitution of leucine for tryptophan 412 does not abolish cytochalasin B labeling but markedly decreases the intrinsic activity of GLUT1 glucose transporter. *J. Biol. Chem.* 266:7769–7773.

Lupas, A., A. J. Koster, J. Walz, and W. Baumeister 1994. Predicted secondary structure of the 20 S proteasome and model structure of the putative peptide channel. *FEBS Lett.* 354:45–49.

Miller, S., J. Janin, A. M. Leak, and C. Chothia. 1987. Interior and surface of monomeric proteins. *J. Mol. Biol.* 196:641–656.

Monge, A., R. A. Friesner, and B. Honig. 1994. An algorithm to generate low-resolution protein tertiary structures from knowledge of secondary structure. *Proc. Natl. Acad. Sci. USA.* 91:5027–5029.

Montal, M. 1990. Molecular anatomy and molecular design of channel proteins. *FASEB J.* 4:2623–2633.

Mueckler, M. 1994. Facilitated glucose transporters. *Eur. J. Biochem.* 219:713–725.

Mueckler, M., C. Caruso, S. A. Baldwin, M. Panico, I. Blench, H. R. Morris, W. J. Allard, G. E. Lienhard, and H. F. Lodish. 1985. Sequence and structure of a human glucose transporter. *Science.* 229:941–945.

Mueckler, M., W. Weng, and M. Kruse. 1994. Glutmine 161 of GLUT1 glucose transporter is critical for transport activity and exofacial ligand binding. *J. Biol. Chem.* 269:20533–20538.

Perutz, M. F. 1985. The pKa values of two histidine residues in human haemoglobin, the Bohr effect, and the dipole moments of alpha-helices. *J. Mol. Biol.* 183:491–498.

Presnell, S. R., and F. E. Cohen. 1989. Topological destribution of four alpha-helix bundles. *Proc. Natl. Acad. Sci. USA.* 86:6592–6596.

Rampal, A. L., E. K. Y. Jung, J. J. Chin, M. R. Dezel, H. B. Puikofsky, and C. Y. Jung. 1986. Further characterization and chemical purity assessment of the human erythrocyte glucose transporter preparation. *Biochim. Biophys. Acta.* 859:135–142.

Robinson, C. R., and S. G. Silgar. 1993. Electrostatic stabilization in four helix bundle proteins. *Protein Sci.* 2:826–837.

Sheridan, R. P., R. M. Levy, and F. R. Salemme. 1982. Alpha-helix dipole model and electrostatic stabilization of four-alpha-helical proteins. *Proc. Natl. Acad. Sci. USA.* 79:4545–4549.

Shoemaker, K. R., P. S. Kim, D. N. Brems, S. Marqusee, and E. J. York. 1985. Nature of the charged-group effect on the stability of the C-peptide helix. *Proc. Natl. Acad. Sci. USA.* 82:2349–2353.

Tamori, Y., M. Hashiramoto, A. E. Clark, H. Mori, A. Muraoka, T. Katowaki, G. D. Holman, and M. Kasuga. 1994. Substitution at Pro 385 of GLUT1 perturbs the glucose transport function by reducing conformational flexibility. *J. Biol. Chem.* 269:2982–2986.

Unwin, N. 1993. Nicotinic acetylcholine receptor at 9A resolution. *J. Mol. Biol.* 229:1101–1124.

Vega, M. C., C. Aleman, E. Giralt, and J. J. Perez. 1992. Conformational study of a nine residue fragment of the antigenic loop of foot-and-mouth disease virus. *J. Biomol. Struct. Dyn.* 10:1–13.

Verlet, L. 1967. Computer experimeents on classical fluids. I. Thermodynamic properties of Lennard-Jones molecules. *Physiol. Rev.* 159: 98–103.

Vriend, G., and V. Eijsink. 1993. Prediction and analysis of structure, stability and unfolding of thermolysin-like proteases. *J. Comput. Aided Mol. Des.* 7:367–396.

Wada, A. 1976. The alpha-helix as an electric macro-dipole. *Adv. Biophys.* 9:1–63.

Wellner, M., I. Monden, M. M. Mueckler, and K. Keller. 1995. Functional consequences of proline mutations in the putative transmembrane segments 6 and 10 of the glucose transporter GLUT1. *Eur. J. Biochem.* 227:454–458.

Williams, S. A., and M. J. Birnbaum. 1988. The rat facilitated glucose transporter gene. Transformation and serum-stimulated transcription initiate from identical sites. *J. Biol. Chem.* 263:19513–19518.